Condensation in Microchannels – Surface Tension Dominated Regime

H S Wang *, John W Rose *

* Corresponding authors: Tel.: ++44 (0)20 78827921; ++44 (0)20 78825275 Fax: ++44 (0)20 89831007;
Email: h.s.wang@qmul.ac.uk; j.w.rose@qmul.ac.uk
School of Engineering and Materials Science, Queen Mary, University of London, UK

Abstract A theoretical model, developed by the authors, for condensation in microchannels takes account of the effects of gravity, streamwise shear stress on the condensate surface as well as the transverse pressure gradient due to surface tension in the presence of change in condensate surface curvature. Numerical results have been generated for various channel shapes, dimensions and inclinations and for various fluids, vapour-to-surface temperature differences and vapour mass fluxes. It is found that, over a certain length of channel, the local mean (around the channel perimeter) heat-transfer coefficient is essentially independent of gravity (including inclination of the channel) and surface shear stress and depends only on surface tension. For the surface tension dominated regime an equation for the Nusselt number, as a function of a single dimensionless group analogous to that occurring in the simple Nusselt theory except that the gravity is replaced by surface tension, has been derived both on the basis of dimensional analysis and by approximate theory. The equation represents all of the data satisfactorily.

Keywords: Condensation, Microchannel, Surface Tension, Refrigerant, Heat Exchanger

1. Introduction

Refrigeration and air conditioning, account for a significant proportion of electricity usage, and consequently for fuel consumption and associated CO_2 emissions. Improvement in design and performance of refrigeration plant can make a significant contribution to mitigation of these problems. Condensers employing microchannel tubes such as those shown in Fig. 1 have been used successfully in automotive air conditioners for around 20 years and have proved both compact and effective.

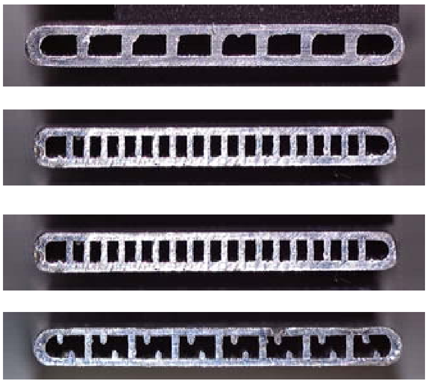

Fig. 1 Multi-port extruded tubes Koyama et al. (2003a, b). Typical channel dimension around 1 mm.

Available experimental heat-transfer data for condensation in microchannels are relatively few and widely scattered. Vapour-side, heat-transfer coefficients have, with a few exceptions (Koyama et al. (2003a,b), Cavallini et al. (2003, 2004, 2006)) generally been inferred from overall measurements by subtraction of thermal resistances and/or using “Wilson plot” techniques; such data generally have high uncertainty. Four correlations based on data for R134a (Wang et al. (2002), Koyama et al. (2003b), Cavallini et al. 2003, 2004), Bandhauer et al. (2006)) have been proposed. The four correlations agree quite well with each other when applied to R134a but wide differences (up to a factor of around four) are found when applied to ammonia (see Su et al. (2009)).

Wang and Rose (2005) developed a theory of condensation in microchannels based on the assumptions of Nusselt but including the streamwise shear stress on the condensate film surface and, most importantly for non-circular channels, the transverse pressure gradient due to surface tension in the presence of curvature of the condensate surface. In the Wang and Rose (2005) theory the differential equation for the condensate film thickness, based only on the Nusselt assumptions as indicated above, is valid to the same degree as in the Nusselt theory for condensation on a plane surface or horizontal tube. However, in order to solve the equation an estimate of the streamwise shear stress on the condensate surface is required. In the solutions obtained to date this has been obtained using standard approximate methods (see Cavallini et al. (1999)) which take account surface transpiration (condensation). The model has been used to predict a wide range of results for typical conditions. Results are found to be only marginally affected by moderate arbitrary changes in the streamwise shear stress so that the accuracy of the streamwise shear stress estimate is of secondary importance.

An interesting finding is that the solutions show, for a range of positions along a channel, that the average (around the channel perimeter) heat-transfer coefficient, α_z, is essentially independent of gravity and distance along the channel but is strongly dependent on surface tension (see Fig. 2). Moreover, increase in vapour mass flux, and hence shear stress on the condensate surface, does not increase the heat-transfer coefficient in this region but rather increases the length of channel over which the heat-transfer coefficient remains essentially constant (see Fig. 3). In this regime it appears that the transverse surface tension driven flow towards the corners dominates over both gravity and streamwise shear stress.

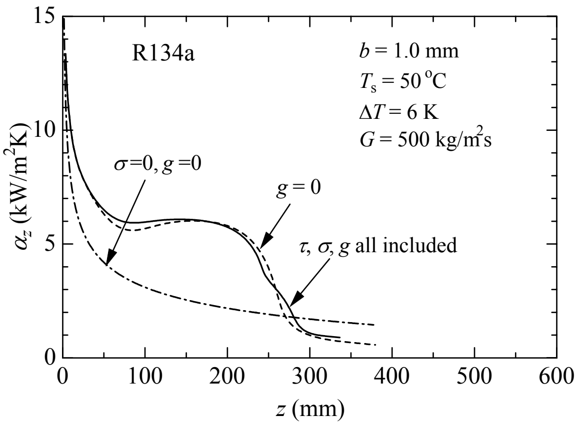

Fig. 2 Mean heat-transfer coefficient for upright equilateral triangular channel (Wang and Rose (2005)).

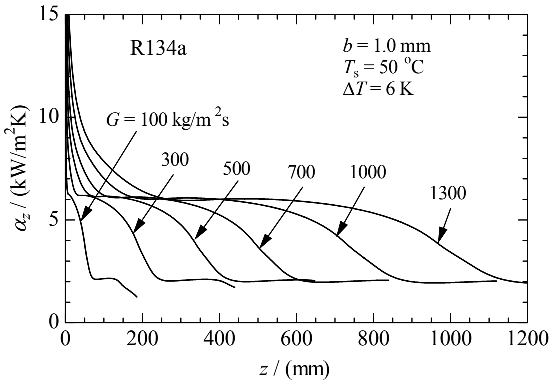

Fig. 3 Mean heat-transfer coefficient along square channel for different vapour mass fluxes (Wang and Rose (2005)).

Figure 4 shows results for different vapour-to-surface temperature differences for a square channel. It is seen, that the heat-transfer coefficient is higher at low ΔT as expected owing to lower condensation rates and consequently thinner condensate films. It is also seen that the range of distance from the channel inlet z over which the heat-transfer coefficient is essentially independent of z is larger at lower ΔT. Figure 5 gives results for square channels of different size. Regions where the heat-transfer coefficient is essentially independent of gravity are identifiable for channels with side 2 mm or smaller. For larger channels it appears that the transverse surface tension effect is small. The heat-transfer coefficient where surface tension dominates increases strongly with decrease in channel dimension while the distance over which the coefficient remains high decreases with decreasing size due to flooding of the channel.

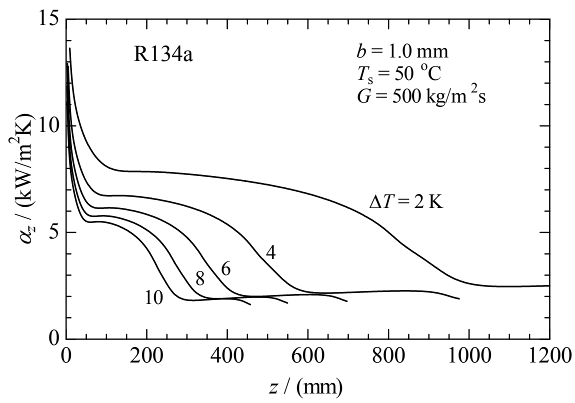

Fig. 4 Mean heat-transfer coefficients for square channel at different vapour-to-surface temperature differences (Wang and Rose (2005)).

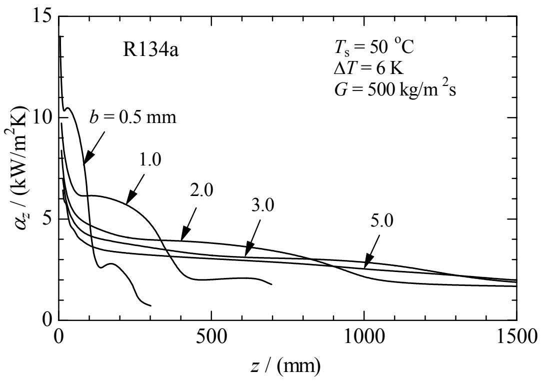

Fig. 5 Mean heat-transfer coefficients for square channels of different size (Wang and Rose (2005)).

Figure 6 shows results for different channel inclinations. Again a range of inclinations can be seen where the heat-transfer coefficient is essentially independent of on inclination for some distance along the channel. Figure 7 gives results for various fluids showing in all cases a range of distance where the heat-transfer coefficient is almost constant. This is least evident, but discernable, for carbon dioxide at around z = 80 mm.

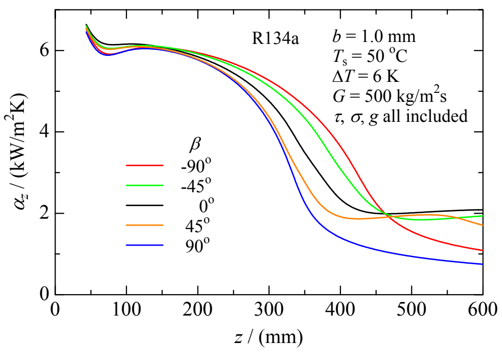

Fig. 6 Mean heat-transfer coefficient for different channel inclinations - negative angles indicate downflow (Wang and Rose (2006))

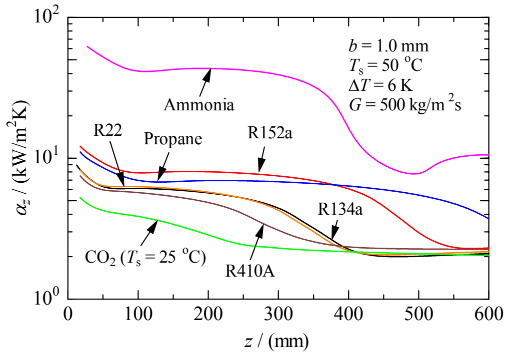

Fig. 7 Mean heat-transfer coefficient for different fluids in square channels. Wang et al. (2007).

2. Dimensional analysis for the surface tension dominated part of the channel

As in the simple Nusselt problem inertia effects in the film are neglected so that the effective mean condensate film thickness is governed by surface tension, viscosity and the rate at which liquid condenses on unit area of the surface V, thus

$$\delta = \psi(\sigma, \mu, x, V) \tag{1}$$

where x is the relevant linear dimension.

Dimensional analysis then gives

$$\frac{\delta}{x} = \varphi\left(\frac{\sigma}{\mu V}\right) \tag{2}$$

We now suppose, as is often done when correlating heat-transfer data, that this function takes the form

$$\frac{\delta}{x} = A\left(\frac{\sigma}{\mu V}\right)^p \tag{3}$$

where A and p are constants.

Then, as in Nusselt, we neglect convection in the condensate film and write

$$V = \frac{m}{\rho} = \frac{q}{\rho h_{fg}} = \frac{\lambda \Delta T}{\delta \rho h_{fg}} \tag{4}$$

Substituting for V in equation (3) and rearranging gives

$$Nu = \frac{q x}{\lambda \Delta T} = C\left(\frac{\rho h_{fg} \sigma x}{\mu \lambda \Delta T}\right)^n \tag{5}$$

where $C = A^{1/(p-1)}$ (6)

and $n = p/(p-1)$ (7)

For the case of the triangular and square channel the relevant linear dimension is the side of the channel b so we have

$$Nu = C\left(\frac{\rho h_{fg} \sigma b}{\mu \lambda \Delta T}\right)^n \tag{8}$$

Values of the heat-transfer coefficient for the surface tension controlled region have been identified as closely as possible from all of the results obtained to date (7 fluids, 7 channel geometries, 5 values of ΔT in the range 2 – 10 K). The corresponding logarithmic plot of Nu against $\rho h_{fg}\sigma b/\mu\lambda\Delta T$ is shown in Fig. 8. (For rectangular channels the geometric mean of the lengths of the two sides was used for b.) A straight line least squares fit gave a value of n very close to 0.25; n was therefore set to this value and the constant C redetermined. The data are evidently satisfactorily represented by

$$Nu = 1.43\left(\frac{\rho\, h_{fg}\sigma\, b}{\mu\,\lambda\,\Delta T}\right)^{1/4} \tag{9}$$

which may be compared with the Nusselt equation for gravity-controlled condensation on a vertical flat plate

$$Nu = 0.943\left(\frac{g\Delta\rho\, h_{fg} L^3}{\mu\,\lambda\,\Delta T}\right)^{1/4} \tag{10}$$

where L is the plate height.

3. Approximate analytical treatment for surface tension-dominated region

For laminar flow of the condensate film, governed only by the pressure gradient due to surface tension in the presence of surface curvature and viscous forces, the Nusselt approximations give the momentum balance equation for transverse flow:

$$\frac{\partial}{\partial y}\left(\mu\frac{\partial u}{\partial y}\right) = \frac{\mathrm{d}P}{\mathrm{d}x} \tag{11}$$

For uniform viscosity, integration with boundary conditions of transverse shear stress zero at the film-vapour interface and velocity zero at the channel wall, gives

$$u = \frac{1}{\mu}\left(\frac{y^2}{2} - \delta\, y\right)\frac{\mathrm{d}P}{\mathrm{d}x} \tag{12}$$

Equating the increase in x-direction mass flow in the film to the mass condensation rate on the surface of an element, as in Nusselt, gives the condensation mass flux

$$m = -\frac{\rho}{3\mu}\frac{\mathrm{d}}{\mathrm{d}x}\left(\delta^3\frac{\mathrm{d}P}{\mathrm{d}x}\right) \tag{13}$$

Neglecting convection in the film we have

$$m = \frac{q}{h_{\mathrm{fg}}} = \frac{\lambda\,\Delta T}{\delta\, h_{\mathrm{fg}}} = -\frac{\rho}{3\,\mu}\frac{\mathrm{d}}{\mathrm{d}x}\left\{\delta^3\frac{\mathrm{d}P}{\mathrm{d}x}\right\} \tag{14}$$

so

$$\frac{\mathrm{d}}{\mathrm{d}x}\left\{\delta^3\frac{\mathrm{d}P}{\mathrm{d}x}\right\} = -\frac{3\mu\,\lambda\,\Delta T}{\rho\, h_{\mathrm{fg}}}\cdot\frac{1}{\delta} \tag{15}$$

Up to equation (15) no assumptions or approximations other than those of Nusselt have been used. We now follow Fujii et al. (1985) and Rose (2002) in their treatment of condensation on wire-wrapped tubes. Where the film is very thin, although change in its surface curvature gives rise to the pressure gradient which drives the transverse flow, for the purposes of integrating Eq. (15) δ is taken to be constant where $x < s/2$ and to take the form of a circular arc of radius r^* when $x > s/2$ (see Fig. 9). Integration of equation (15) with $\mathrm{d}P/\mathrm{d}x = 0$ at $x = 0$ by symmetry, gives

$$\frac{\mathrm{d}P}{\mathrm{d}x} = -\frac{3\mu\,\lambda\,\Delta T\, x}{\rho\, h_{\mathrm{fg}}\,\delta^4} \tag{16}$$

Integration of equation (16) across the slope discontinuity at $x = s/2$, together with delta-function behaviour of the pressure gradient at $x = s/2$, gives:

$$P_{s/2} - P_0 = -\frac{3\mu\; k\,\Delta T\,(s/2)^2}{2\,\rho\; h_{\mathrm{fg}}\;\sigma\,\delta^4} = -\frac{\sigma}{r^*} \tag{17}$$

Then

$$\delta^4 = \frac{3\,\mu\, k\,\Delta T\, r^*\, s^2}{8\,\rho\, h_{\mathrm{fg}}\sigma} \tag{18}$$

The heat flux along s is given by

$$q_{\mathrm{s}} = \frac{\lambda\,\Delta T}{\delta} \tag{19}$$

and over the whole of the channel side by

$$q = q_{\mathrm{s}}\, s / b \tag{20}$$

Neglecting heat transfer through the thick film at the corners. Thus the Nusselt number for the channel side is

$$Nu = \frac{q\,b}{\Delta T\,\lambda} = \frac{q_s\,s}{\Delta T\,\lambda} = \frac{s}{\delta} = \left(\frac{8\,\rho\,h_{fg}\sigma\,s^2}{3\mu\,\lambda\,\Delta T\,r^*}\right)^{1/4} \quad (21)$$

Neglecting the film thickness except at the corners gives

$$s = b - 2r^* \quad (22)$$

for a square section channel

$$s = b - 2\sqrt{3}\,r^* \quad (23)$$

for an equilateral triangular section channel

so that

$$Nu = C\left(\frac{\rho\,h_{fg}\,\sigma\,b}{\mu\,\lambda\,\Delta T}\right)^{1/4} \quad (24)$$

$$C = \left\{\frac{8}{3}\left(\xi + \frac{4}{\xi} - 4\right)\right\}^{1/4} \quad (25)$$

for a square channel

and

$$C = \left\{\frac{8}{3}\left(\xi + \frac{12}{\xi} - 4\sqrt{3}\right)\right\}^{1/4} \quad (26)$$

for a triangular section channel

where

$$\xi = b\,/\,r^* \quad (27)$$

It is not clear how one should estimate values r^* from the film profiles. Examination of profiles for square and triangular duct, at positions along the channel where the heat-transfer coefficient was essentially constant (see Fig. 10), indicated values s, r^* and ξ leading to values of C between 1 and 2. The values obtained depended on judgement of what should be considered as the thin film region (value of s) and also somewhat on the vapour mass flux and the side of the channel used for measurement. The range values obtained for C is evidently in accord with 1.43 found from the dimensionless heat-transfer plot Fig. 8.

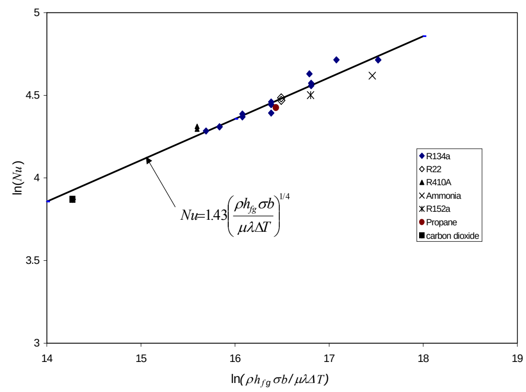

Fig. 8 Correlation of results for surface tension dominated region

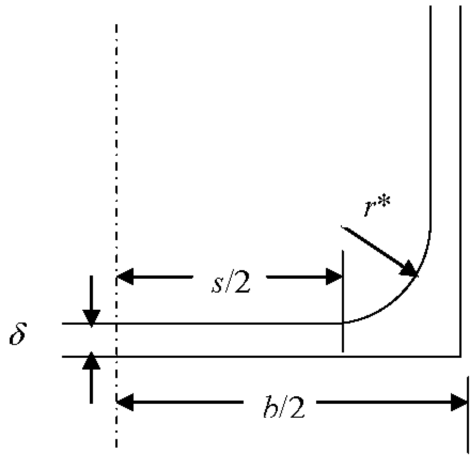

Fig. 9 Approximate film profile for integration of Eq. 15

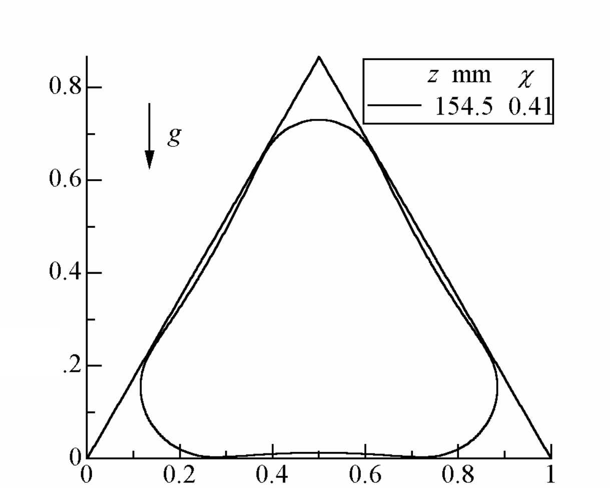

Fig. 10 Calculated condensate film profiles in the surface tension dominated region. Horizontal channels, channel side b = 1 mm, G = 500 kg/m^2 s (Wang and Rose (2005)).

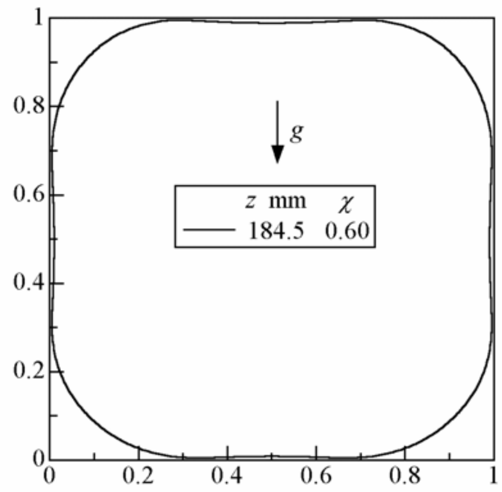

Fig. 10 (continued)

4. Conclusion

For condensation in sufficiently small channels, solutions of the differential equation for the annular flow regime indicate ranges of the relevant variables where the transverse flow, due to the pressure gradient resulting from surface tension in the presence of changing surface curvature, dominates over gravity and shear stress. For this regime, numerically obtained heat-transfer coefficients, for a wide range of circumstances, are satisfactorily correlated by a simple equation analogous to the Nusselt result for gravity-controlled condensation.

The present simple result is a first step towards the goal of summarizing all of the theoretical results in the form of simple algebraic equations for ready use in design and optimization. In view of the fact that the heat-transfer coefficient is higher upstream of the surface tension dominated region and lower downstream, the present result may perhaps give a useful order-of-magnitude estimate of the heat-transfer coefficient for the channel as a whole for any fluid, geometry and temperature difference.

Nomenclature

A	constant, see Eqn. (3)
b	length of side of channel
C	constant, see Eqns. (5) and (24)
G	mass flux of vapour
g	specific force of gravity
h_{fg}	specific enthalpy of evaporation
L	plate height in simple Nusselt theory
m	condensation mass flux
Nu	Nusselt number, see Eqs. (5) and (24)
n	constant, see Eqn. (8)
P	pressure in condensate film
p	constant, see Eqn. (3)
q	heat flux
r^*	radius of condensate film in corner in approximate analysis, see Fig. 9
s	thin film region of channel side, see Fig. 9
T_s	temperature of channel surface
V	volume condensation flux on condensate surface
x	coordinate measured from the top centre along channel side; linear dimension, see Eqn. (1)
y	coordinate normal to channel side.
z	distance along channel

Greek symbols

α_z	average heat-transfer coefficient over perimeter of channel at location z
β	channel inclination to vertical
δ	condensate film thickness
ΔT	vapour-surface temperature difference
λ	condensate thermal conductivity
μ	condensate viscosity
ξ	b/r^*
ρ	condensate density
σ	surface tension
τ	vapour shear stress at vapour-liquid interface
χ	mass quality

References

Bandhauer, T. M., Agarwal, A. and Garimella, S., (2006), Measurement and modelling of condensation heat transfer coefficients in circular microchannels, ASME Journal of Heat Transfer, **128**(10), 1050-1059.

Cavallini, A., Del Col, D., Doretti, D., Longo, G. A. and Rossetto, L. (1999), A new computational procedure for heat transfer and pressure drop during refrigerant condensation inside enhanced tubes, J. Enhanced Heat Transfer, **6**. 441-446.

Cavallini, A., Censi, G., Del Col, D., Doretti, L., Longo, G. A., Rossetto, L. and Zilio, C., (2003), Experimental investigation on condensation heat transfer coefficient inside multi-port minichannels, 1st Int. Conf. on Microchannels and Minichannels, Rochester, 691-696.

Cavallini, A., Del Col, D., Doretti, L., Matkovic, M., Rossetto, L. and Zilio, C., (2004), Condensation heat transfer inside multi-port minichannels, 2nd Int. Conf. on Microchannels and Minichannels, Rochester, 625-632.

Cavallini, A., Del Col, D., Matkovic, M. and Rossetto, L., (2006), Measurement of local heat transfer coefficients during condensation of R134a inside a single circular minichannels*,* Proc. Int. Conf. on Heat Transfer, Sydney, Australia. Aug. 13-18.

Fujii, T, Wang, W.C., Koyama, S and Shimuzu, Y (1985). Heat transfer enhancement for gravity controlled condensation on a horizontal tube by coiling wires. Proc. 2nd Int. Symp. Heat Transfer, Tsinghua Univ., Beijing, Oct. 15-18, 1995, and in Heat Transfer Science and Technology, Ed. Bu-Xuan Wang, Hemisphere 1987, pp. 773-780.

Koyama, S., Kuwahara, K. and Nakashita, K., (2003a), Condensation of refrigerant in a multi-port channel, 1st Int. Conf. on Microchannels and Minichannels, Rochester, 193-205.

Koyama, S., Kuwahara, K., Nakashita, K. and Yamamoto, K., (2003b), An experimental study on condensation of refrigerant R134a in a multi-port extruded tube, *Int. J. Refrigeration*, **24**, 425-432.

Rose, J. W. (2002). An analysis of film condensation on a horizontal wire-wrapped tube. *Trans. IChemE* **80**, Part A pp. 290-294.

Wang Wei-Wen, W., Radcliff, T. D. and Christensen, R. N., (2002), A condensation heat transfer correlation for millimetre-scale tubing with flow regime transition, *Experimental Thermal and Fluid Science*, **26**, 473-485.

Wang, H. S. and Rose, J. W. (2005). Film condensation in microchannels – a theoretical model for rectangular section. *Trans. ASME J. Heat Transfer*, **127**, 1096-1105.

Wang, H. S. and Rose, J. W. (2006), Film condensation in microchannels: effect of tube inclination. Proc. Fourth ASME International Conference on Nanochannels, Microchannels and Minichannels. June 19-21, 2006 Limerick, Ireland. Paper ICNMM2006-96049.

Su, Q., Yu, G. X., Wang, H. S. and Rose, J. W. (2009), Microchannel Condensation: theory and correlations, *Int J. Refrigeration*. In press

Wang, H. S. Ding, J and Rose, J. W. (2007). Heat transfer during annular film condensation in microchannels: calculations for R152a, R134a, R22, R410, propane, ammonia and carbon dioxide. Proc. 6th Int. Conf. on enhanced, compact and ultra compact heat exchanger: ECI. Potsdam, 12-16 September, 2007.